Surface resistance of the heavy-fermion superconductor UPt_3

C. C. Grimes, G. Adams, and E. Bucher
AT&T Bell Laboratories, Murray Hill, New Jersey 07974
(Received 17 December 1990)

The surface resistance R of two UPt_3 single crystals has been measured using an apparatus in which the direction of the rf or microwave current can be varied continuously relative to the crystal axes. In an a-axis single crystal at 0.38 K, R is found to be lower for current in the basal plane than for current along the c axis, while R is independent of current direction in a c-axis crystal. This suggests that the superconducting-energy-gap function is anisotropic with, on average, a larger gap in basal-plane directions than in the c-axis direction. R at 0.38 K is found to increase anomalously rapidly with increasing frequency to nearly the normal-state value at frequencies that are only a few percent of kT_c.

INTRODUCTION

There is strong evidence that the heavy-fermion superconductor UPt_3 has an unconventional superconducting ground state.[1] Power-law temperature dependences of the low-temperature specific heat[2] and longitudinal ultrasonic attenuation[3] have been attributed to a gap function that has nodes. Dependence of the transverse ultrasonic attenuation on polarization[4] has been interpreted as direct evidence for an anisotropic superconducting ground state.[5] More recently, a second peak has been observed in the low-temperature specific heat below T_c indicating a second superconducting phase transition which could only occur if the pairing were unconventional.[6] Ultrasonic attenuation,[7,8] specific heat,[9] and mechanical measurements of the flux lattice[10] reveal a complex phase diagram in the (H,T) plane with three distinct superconducting phases indicative of unconventional superconductivity.

To gain insight into the nature of its superconducting states, we have studied the surface resistance of UPt_3 single-crystal specimens using an apparatus in which the direction of the rf or microwave current can be varied continuously relative to the crystal axes. This study was motivated by calculations which indicated that in a single crystal, single domain specimen at temperatures well below the transition temperature and at finite frequencies, the surface resistance is larger when the current is in a direction in which the gap function vanishes than it is for an arbitrary direction.[11,12] Hence, this experiment has the potential of mapping out the directions in which the gap function has points or lines of zeros and can thereby provide detailed microscopic information about the anisotropy of the superconducting states.

This paper presents our measurements of the surface resistance of UPt_3. A detailed interpretation of our experimental results is not attempted; for works by Klemm *et al.* and Hirschfeld *et al.* have shown that extensive calculations are needed to interpret surface resistance measurements in detail.[11,12] However, the qualitative indications from our data are that in the highest temperature superconducting phase, the energy gap in UPt_3 (which has hexagonal crystal structure) is, on average, larger in the basal plane than in the c-axis direction.

Below we describe our experimental apparatus, and we describe how the specimens were prepared and mounted. Then we present our experimental results, a discussion of the results, and the conclusions from this work.

APPARATUS

We have employed a calorimetric technique to measure the surface resistance, R. We determine the temperature rise of the specimen while it is exposed to rf or microwave radiation, then with the microwave power off, measure the amount of electrical power that must be applied to a heater to reproduce that temperature rise. The measurement is thus reminiscent of the pioneering study by Biondi and Garfunkel on superconducting Al.[13]

A schematic drawing of our microwave calorimeter is shown in Fig. 1. In this apparatus the rf or microwave current is induced in the specimen's surface by a rotatable hairpin-shaped loop spaced ≈ 0.02 cm above the flat specimen. This hairpin loop is ≈ 0.4 cm long and ≈ 0.09 cm wide. It terminates a 75-Ω coaxial line, the last 3 cm of which can be rotated via a set of gears and a shaft that extends through the top of the cryostat. Rotation of the coaxial line and its hairpin loop then rotates the direction of the microwave current induced in the specimen. The critical problem in designing such a microwave calorimeter is to provide good thermal contact between the specimen and a thermometer while isolating the thermometer from microwave radiation which is incident on the specimen. These objectives are achieved in our apparatus by employing as "thermal links" single-crystal quartz bars passing through tunnels in a copper block. The quartz bars have square (0.064×0.064 cm^2) cross sections and are carefully centered in the tunnels whose cross sections are 0.079×0.079 cm^2. The microwave dielectric constant of single-crystal quartz is ≈ 4.5, so each thermal link is electrically equivalent to a wave guide which is beyond cut-off for frequencies below ≈ 110 GHz. The specimen

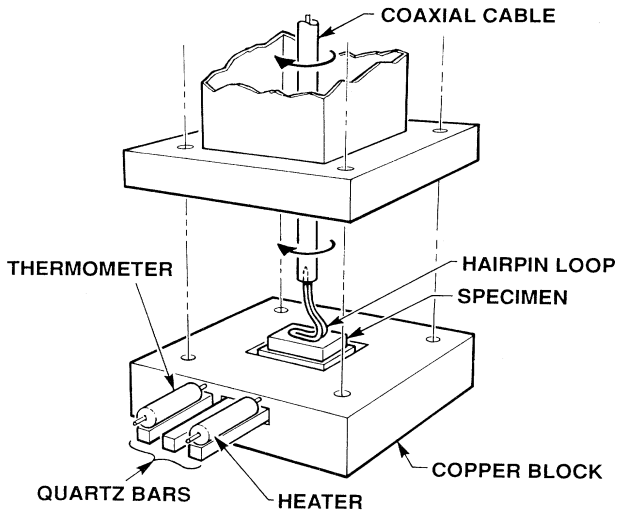

FIG. 1. Schematic diagram of the microwave calorimeter. The direction of the microwave current induced in the surface of the specimen is varied by rotating the coaxial cable and hairpin loop.

is glued to a single-crystal quartz plate to which three of the above-described thermal links are bonded. One thermal link connects to a resistance thermometer, another connects to a heater, and the third connects to the thermal ground. For all frequencies below 110 GHz the thermometer and heater are well isolated from the microwave radiation incident on the specimen. The microwave calorimeter is attached to a continuous circulation ^{3}He refrigerator which can cool to 0.37 K. A feedback loop maintains the thermal ground at a constant temperature during measurements.

One problem encountered with this apparatus arose from the mechanism used to rotate the hairpin loop. We employed a 0.24-cm-diam thin wall stainless-steel tube 168 cm long to drive the gear train in the cryostat from a knob at the top of the dewar. Although this mechanism rotated freely when the whole apparatus was at room temperature, it sometimes was sticky and/or hysteretic when cold. This appeared to be due to residual gases freezing onto the shaft support bushings during the cooldown procedure. To minimize the effects of hysteresis, the shaft was rotated by fixed increments in only one direction when taking data.

SPECIMENS

The single-crystal UPt_3 specimens studied in this work were cut from a single-crystal boule grown by the floating zone method. The boule was ≈ 0.43 cm in diameter and a few cm long. The growth direction was with the c axis along the axis of the boule. Palstra has measured the dc resistivity of a specimen cut from the same boule.[14] He found the resistivity extrapolated to $T=0$ to be approximately 3.7 $\mu\Omega$ cm for current in the basal plane. Combining this with the room-temperature resistivity yields a residual resistivity ratio of ≈ 89. Ramirez measured the ac susceptibility of one of our specimens and found the T_c for onset of superconductivity to be 0.525 K and the 10–90 % transition width to be 0.050 K.[15]

Specimens in the form of square plates $\approx 0.4 \times 0.4 \times 0.1$ cm^3 having the c axis either in the plane of the plate or normal to it were cut from the boule using a diamond impregnated wire saw. The square faces of the specimens were successively lapped with 5 and then 0.5 μm alumina powder, and then chemically etched in dilute aqua regia to remove the damaged surface layer. The specimens were then annealed in vacuum at 1340 °C and slowly cooled. Backreflection x-ray Laue photographs revealed that the surfaces were essentially strain free, and each specimen had the intended orientation within $\approx 1°$. The oriented specimen was attached to the calorimeter with a tiny drop of GE7031 cement.

RESULTS

The quantity determined in our experiments is the surface resistance ratio $R_s(T)$ which is the surface resistance measured at temperature T divided by the surface resistance measured at $T=0.7$ K. We have chosen 0.7 K as a reference temperature because it is conveniently close to, but above, T_c for UPt_3. In Fig. 2 we show a family of $R_s(T)$ curves obtained at three different frequencies in a specimen having the c axis perpendicular to its planar surface. (We will refer to this specimen as the c-axis specimen or as the basal-plane specimen.) At the lowest frequency, 10 MHz, $R_s(T)$ drops rapidly below 0.50 K indicating the onset of superconductivity at that temperature. At 10 MHz the value of $R_s(T)$ drops to 0.01 at 0.38 K. As the frequency is increased, the apparent onset

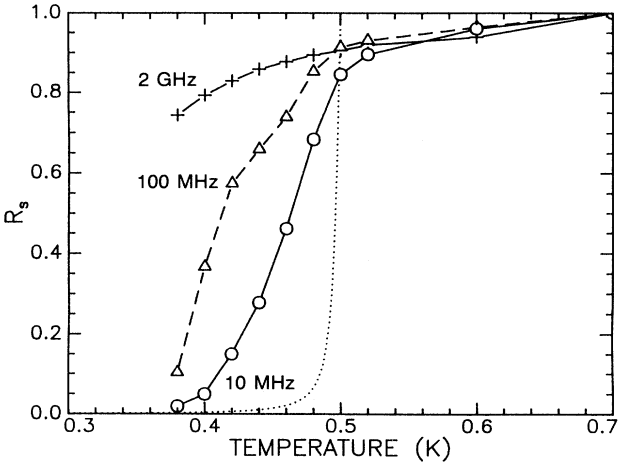

FIG. 2. R_s, the ratio of the surface resistance at temperature T to that at $T=0.7$ K, plotted vs temperature. The hexagonal single crystal has its c axis perpendicular to the surface, so the measuring current is flowing in the basal plane. The dotted line represents the calculated surface resistance at 2 GHz for a conventional superconductor having $T_c=0.5$ K.

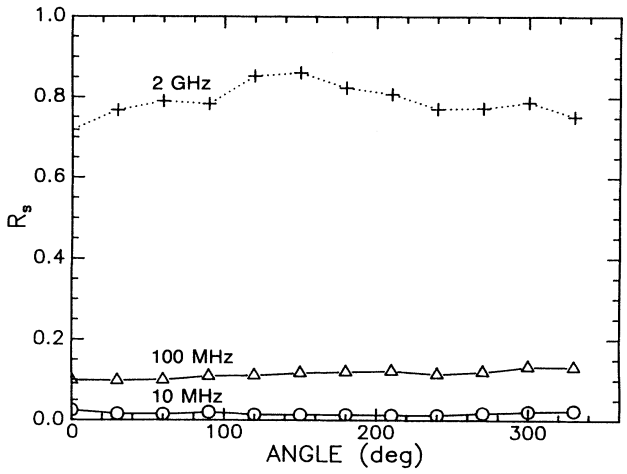

FIG. 3. Surface resistance ratio, R_s (0.38 K), for the same specimen as in Fig. 2 plotted vs the direction of the measuring current relative to the crystal axes in the basal plane.

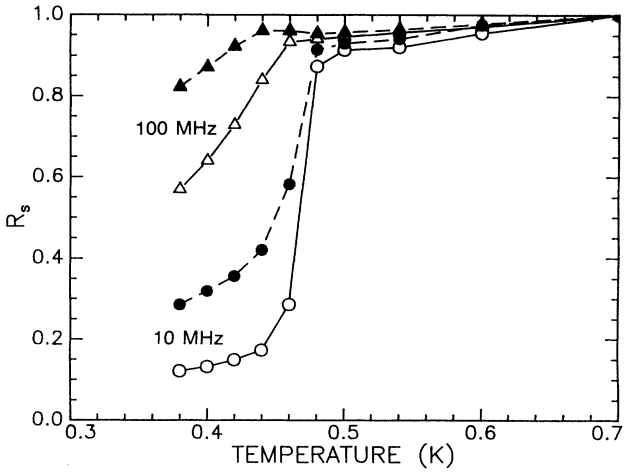

FIG. 5. R_s, as in Fig.2, plotted against temperature for two different directions of the current in the a-plane specimen. The solid symbols denote rf current in the c-axis direction while the open symbols denote rf current perpendicular to the c axis.

temperature decreases and $R_s(T)$ decreases more slowly with decreasing T. The shoulder at 0.42 K on the 100-MHz curve is the only indication in our data of a possible second superconducting transition which has been seen by others.

In the basal-plane specimen the value of R_s (0.38 K) does not vary significantly with the direction of the ac current relative to the crystal axes. This is illustrated in Fig. 3. However, in a specimen having an a axis perpendicular to its surface so the c axis lies in the plane of the specimen, R_s (0.38 K) does vary with the angle, θ, between the ac current and the c axis. This is illustrated in Fig. 4. At 10 and 100 MHz, R_s (0.38 K) is a minimum when the current is in the basal plane and a maximum when the current is along the c axis. At 2 GHz there is very little variation of R_s (0.38 K) with current direction. For a conventional s-wave pairing (BCS) superconductor, R_s (0.38 K) would lie practically on the abscissa at all three frequencies. Figure 5 displays the temperature dependence of $R_s(T)$ in the a-plane specimen at 10 and 100 MHz for the two directions corresponding to the current approximately along the c axis and perpendicular to it.

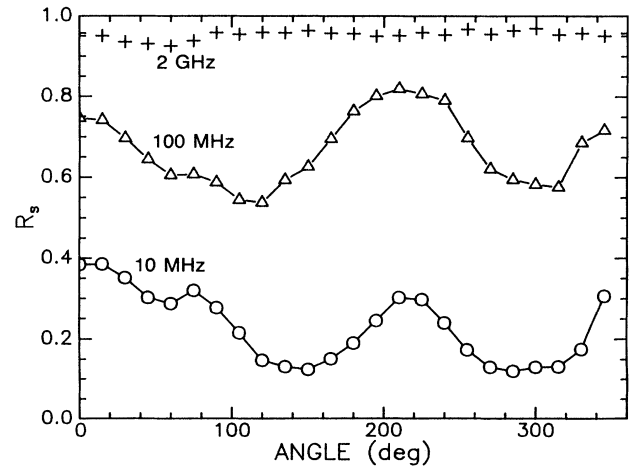

FIG. 4. Surface resistance ratio plotted vs the direction of the measuring current in an a-plane specimen. The current is flowing in the c-axis direction when the abscissa angle is near 0° and again near 220°.

DISCUSSION

The most striking result of this work is the surprisingly rapid increase of R_s with increasing frequency at our lowest temperature of 0.38 K ($T/T_c=0.76$). The behavior displayed in Fig. 2 is quite different than that expected for a BCS superconductor having the same T_c. For a BCS superconductor one would expect R_s to drop rapidly below T_c to a value near zero for all three frequencies because the photon energies are very small relative to the BCS gap energy. The calculated $R_s(T)$ at 2 GHz for a BCS superconductor having $T_c=0.5$ K and a gap $2\Delta=3.5kT_c$ is shown as the dotted curve in Fig. 2. Note that for our highest frequency, 2 GHz, the photon energy is only 0.1 K. The rapid increase of R_s with increasing frequency indicates that even very low-energy photons can excite quasiparticles. Such behavior is consistent with an energy gap function that has nodes.

Raw data displaying the observed variation of R_s with angles are shown in Fig. 4. The angle displayed on the abscissa is the angular position of the knob located at the top of the control shaft. Due to the "binding" and "sticking" problems mentioned above, the actual angle through which the hairpin loop rotated varied each time

the control knob was rotated a given amount. This introduced a lag between the two rotations that produced flat spots as seen near 80° in Fig. 4. Farther along in the sequence of data points, the hairpin loop tended to partially catch up with the position of the knob. This produced steep rises and rapid falls in $R_s(\theta)$. Consequently, variable lag between the two rotations produced the pattern in Fig. 4 that does not display the appropriate symmetry. The pattern should, of course, repeat every 180°. [Below, we show some data taken during a different cool down where sticking was not a problem, and the $R_s(\theta)$ pattern displayed the expected symmetry.]

Palstra's measurements[14] can be extrapolated to yield 4.8 $\mu\Omega$ cm for the dc resistivity in the basal plane at 0.7 K. Assuming that our specimens have approximately the same resistivity, we deduce that the electron mean free path is $l=\approx 3\times 10^{-6}$ cm. The classical skin depth at 2 GHz becomes $\delta\approx 2\times 10^{-4}$ cm. Hence, in the normal state $\delta \gg l$ for all of the frequencies employed in our experiments. This means that the dirty limit or ordinary skin effect conditions apply. The normal-state surface impedance is then given by $Z=R+iX=(1+i)(2\pi\omega\rho/c^2)^{1/2}$ so the surface resistance R increases as $\omega^{1/2}$ and $\rho^{1/2}$.

Klemm *et al.* have calculated the magnetic-field penetration depth, surface resistance, and far-infrared reflectivity for unconventional superconductors.[11] They treated two anisotropic order parameters having either points or lines of nodes in the energy gap, and they took into account resonant impurity scattering for a wide range of scattering rates. For their surface resistance calculations they took the $q_i \rightarrow 0$ limit where the q_i are spatial Fourier components of the fields and currents in the superconductor. This limit should be applicable to our experiment where $\delta > \Lambda > l$. Here Λ is the London penetration depth which Gross *et al.* found to be 1.9×10^{-4} cm.[16] For a uniaxial state having the order parameter either parallel or perpendicular to the surface, the surface resistance has the form

$$R(\theta)=R_1\cos^2\theta+R_2\sin^2\theta\ . \tag{1}$$

We will use this simple form for the surface resistance in what follows where we correct for the fact that our hairpin loop is not ideal and where we take into account the anisotropy of the normal-state resistivity at our reference temperature of 0.7 K.

The hairpin loop described above that induces current in the specimen has an aspect ratio of about 4:1. Consequently, in an isotropic material about 80% of the total microwave dissipation is due to current flowing parallel to the long dimension of the loop and 20% is due to current flowing in the perpendicular direction. This mixing of parallel and perpendicular components partially averages out the anisotropy in surface resistance in an anisotropic material. Assuming that the surface resistance can be expressed in the form (1), it is a simple matter to deduce the intrinsic anisotropy of $R(\theta)$ from the measured quantities.

The anisotropy of the dc resistivity of UPt_3 was determined by de Visser *et al.* in specimens having residual ratios ≈ 79.[17] They found the dc resistivity at 0.7 K was 3.8 $\mu\Omega$ cm in the basal plane and 2.0 $\mu\Omega$ cm along the c-axis direction. Since our specimens have comparable residual resistivity ratios, we assume that the ratio of the c-axis resistivity to basal-plane resistivity is the same in our specimens as in theirs. Recalling that $R\propto\rho^{1/2}$, we take the ratio of the surface resistances at 0.7 K to be $R_c/R_{bp}=0.73$ where the subscripts denote c-axis and basal-plane directions. Since our measured quantity R_s is the ratio of the dissipation in the superconducting state to that in the normal state at 0.7 K, to obtain the surface resistance $R(\theta)$ in the superconducting state, we must multiply $R_s(\theta)$ by the appropriate normal state surface resistance $R_n(\theta)$. Of course, both the dissipation measured in the superconducting state and that measured in the normal state represented partially averaged quantities due to the finite aspect ratio of the hairpin loop as described above.

Returning to Fig. 4 and keeping in mind the problems with the rotation mechanism described above, we extract from the figure just the average of the two maxima and the two minima in R_s for the rotation sequence at 10 and at 100 MHz. Using these values in (1) yields an idealized data curve, $R_s(\theta)$. It is then straightforward to correct for the averaging due to the finite aspect ratio of the hairpin loop. At the same time we can derive the surface resistance normalized to its maximum value in the normal state at 0.7 K taking into account the anisotropy of the resistivity in the normal state. In Fig. 6 the upper (dash-dotted) curve displays the normalized surface resistance $R_n(\theta, 0.7\text{ K})$ calculated from the dc resistivity at 0.7 K. The product of $R_n(\theta,\ 0.7\text{ K})$ and $R_s(\theta)$ corrected for averaging, produces the other two curves in Fig. 6. These curves represent normalized surface resistances at 10 and 100 MHz that would have been derived from measurements using an ideal hairpin loop having an infinite

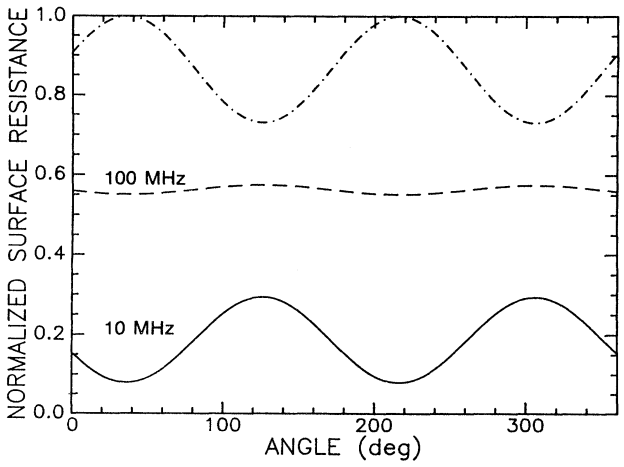

FIG. 6. Surface resistance for the a-plane specimen vs the direction of the measuring current. The upper curve (dashed line) shows the normalized surface resistance calculated for the normal state of UPt_3 at 0.7 K. The lower two curves are idealized curves derived from the maxima and minima in the corresponding data curves in Fig. 4.

aspect ratio. Note that at 2 GHz where the specimen behaves as though it were nearly normal, the surface resistance variations are opposite in phase to those at the lower frequencies where the specimen displays superconducting behavior.

The principal result shown in Fig. 6 is that in the superconducting state at 0.38 K, the surface resistance drops more rapidly with decreasing frequency for current in the basal plane than it does for current along the c axis. From Fig. 3 we found that for all current directions in the basal-plane specimen the 0.38-K surface resistance is smallest and is isotropic. This behavior is qualitatively that which is expected for a state having an average energy gap that is larger in the basal plane than in the c-axis direction. One such state is the axial state which has point nodes in the gap in the c-axis direction. Klemm *et al.* have calculated the surface resistance of an axial state and found behavior qualitatively like that which we observe, but the observed frequencies are more than a factor-of-10 smaller than those in the calculation. Several properties of UPt_3 indicate that its low-temperature gap structure is not axial, but rather a state having one or more lines of nodes.

Other states which have a larger average gap in the basal plane than in the c-axis direction are those which have lines of nodes in planes containing the c axis. The lines of nodes resemble lines of longitude on the globe and intersect at the poles in the c-axis directions. Several singlet d-wave pairing states possess such lines of nodes and some have been proposed as the states assumed by UPt_3.[18] We are not aware of any surface impedance calculations for such states, but it is clear that microwave current in the c-axis direction can excite quasiparticles at all temperatures and frequencies due to the intersecting nodal lines in the gap in that direction. In the basal plane a finite gap develops over a significant fraction of the Fermi surface as T is lowered below T_c, and the surface resistance averaged over all possible domain orientations drops accordingly.

For a state having lines of nodes in planes containing the c axis, domain structure will be important if the order parameter has lower symmetry than hexagonal. For example, if the lines of nodes occur in a pair of orthogonal planes containing the c axis, then there are at least three equivalent orientations of the nodal planes relative to the crystal axes. A multidomain specimen could then appear isotropic in the basal plane in a surface resistance study.

Ambegaokar *et al.* calculated that the direction of the order parameter in the axial state in superfluid ^{3}He would tend to be oriented perpendicular to surfaces.[19] More recently, the boundary conditions applicable at surfaces and interfaces for unconventional superconductors have been reviewed by Kurkijarvi *et al.*[20] If the pair angular momentum in anisotropic superconductors also tends to be oriented perpendicular to surfaces, then such a boundary condition would be satisfied in the c-axis specimen. For this specimen R drops more rapidly with decreasing T and it increases more slowly with increasing frequency than for the a-plane specimen. For the a-plane specimen the order parameter axis would have to bend from the c axis toward the a axis as the surface is approached to satisfy the boundary condition. The effect of such an order parameter texture on the surface resistance has not been explicitly calculated to our knowledge. However, it is plausible to argue that since the bending costs energy, it lowers the gap leading to increased surface resistance. This may be the reason why R_s (0.38 K) is larger for current in the b-axis direction than in the a-axis specimen (i.e., at the minima in the lower curves in Fig. 4) than for current in the same direction in the basal-plane specimen shown in Fig. 3.

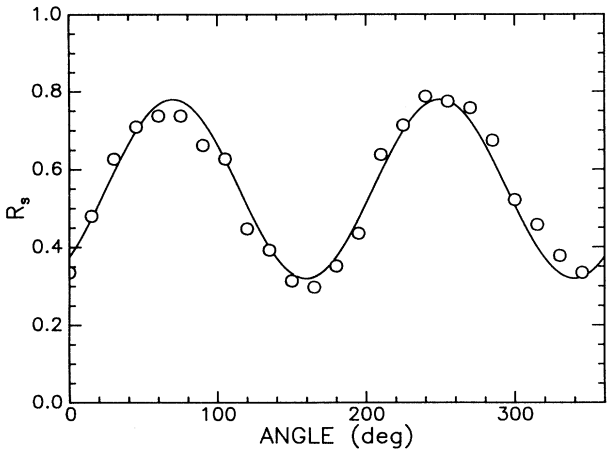

FIG. 7. The data points are measured surface resistance ratios at 10 MHz as in Fig. 4, but with a field of 0.21 T applied parallel to the surface of the specimen. The solid line is the function in Eq. (1) fitted to the data.

Although we have not attempted a detailed study of the behavior of R in a magnetic field, we have applied fields to the a-axis specimen in two different directions. The field strengths employed were greater than H_{c1} (2.2 mT) but much smaller than H_{c2} (2.2 T). The perpendicular field causes R to increase rapidly: a factor of 2.7 in 25 mT.

The surface resistance increases more slowly when a field is applied parallel to the surface. Figure 7 shows a rotation sequence taken for the a-axis specimen with a field of 0.21 T applied in a direction approximately 30° from the c axis. (This was the only orientation of the field and the maximum field strength available with our apparatus.) The rotation mechanism was working well for these data sequences, and $R_s(\theta)$ displays the angular dependence of Eq. (1). The surface resistance is increased by the field, but the anisotropy pattern is not changed in orientation relative to the crystal axes.

CONCLUSIONS

We have observed anisotropy in the surface resistance of an a-axis single-crystal specimen of superconducting UPt_3. The surface resistance at 0.38 K is lower for current in the basal plane than for current in the c-axis direction. This suggests that the energy-gap function is anisotropic with, on average, a larger gap in basal-plane directions than in the c direction. The surface resistance variation with frequency is anomalous. It increases to

nearly the normal-state value at frequencies that are only a few percent of kT_c.

ACKNOWLEDGMENTS

We are indebted to H. Barz for annealing one of the specimens, to A. P. Ramirez for performing a susceptibility measurement, and to A. Kortan for taking x-ray photographs of the specimens. We are grateful to T. Palstra and C. Broholm for providing us unpublished measurements. We have benefited from stimulating discussions with G. Aeppli, D. J. Bishop, E. I. Blount, C. Broholm, R. N. Kleiman, and T. Palstra regarding this work.

[1]For a recent review see P. Wolfle, J. Magn. Magn. Mater. **76&77**, 492 (1988).
[2]G. R. Stewart, Z. Fisk, J. O. Willis, and J. L. Smith, Phys. Rev. Lett. **52**, 679 (1984).
[3]D. J. Bishop, C. M. Varma, B. Batlogg, and E. Bucher, Phys. Rev. Lett. **53**, 1009 (1984).
[4]B. S. Shivaram, Y. H. Jeong, T. F. Rosenbaum, and D. G. Hinks, Phys. Rev. Lett. **56**, 1078 (1986).
[5]S. Schmidt-Rink, K. Miyake, and C. M. Varma, Phys. Rev. Lett. **57**, 2575 (1986); P. Hirschfeld, D. Vollhardt, and P. Wolfle, Solid State Commun. **59**, 111 (1986).
[6]R. A. Fisher, S. Kim, B. F. Woodfield, N. E. Phillips, L. Taillefer, K. Hasselbach, J. Flouquet, A. L. Giorgi, and J. L. Smith, Phys. Rev. Lett. **62**, 1411 (1989).
[7]V. Muller, Ch. Roth, D. Maurer, E. W. Scheidt, K. Luders, E. Bucher, and H. E. Bommel, Phys. Rev. Lett. **58**, 1224 (1987).
[8]Y. J. Qian, M.-F. Xu, A. Schenstrom, H.-P. Baum, J. B. Ketterson, D. Hinks, M. Levy, and B. K. Sarma, Solid State Commun. **63**, 599 (1987).
[9]K. Hasselbach, L. Taillefer, and J. Floquet, Phys. Rev. Lett. **63**, 93 1989.
[10]R. N. Kleiman, P. L. Gammel, E. Bucher, and D. J. Bishop, Phys. Rev. Lett. **62**, 328 (1989).
[11]R. A. Klemm, K. Sharnberg, D. Walker, and C. T. Rieck, Z. Phys. B **72**, 139 (1988).
[12]P. J. Hirschfeld, P. Wolfle, J. A. Sauls, D. Einzel, and W. O. Putikka, Phys. Rev. B **40**, 6695 (1989).
[13]M. A. Biondi and M. P. Garfunkel, Phys. Rev. **116**, 853 (1959).
[14]T.T.M. Palstra (private communication).
[15]A. P. Ramirez (private communication).
[16]F. Gross, K. Andres, and B. S. Chandrasekhar, Physica B+C **162–164C**, 419 (1989).
[17]A de Visser, A. Menovsky, and J.J.M. Franse, J. Magn. Magn. Mater. **63**, 365 (1987).
[18]E. I. Blount, C. M. Varma, and G. Aeppli, Phys. Rev. Lett. **64**, 3074 (1990); D. W. Hess, T. A. Tokuyasu, and J. A. Sauls, Physica B+C **163B**, 720 (1990); R. Joynt, J. Phys. Condens. Matter **2**, 3415 (1990).
[19]V. Ambegaokar, P. G. deGennes, and D. Rainer, Phys. Rev. A **9**, 2676 (1974).
[20]J. Kurkijarvi, D. Rainer, and J. A. Sauls, Can. J. Phys. **65**, 1440 (1987).